1829 Shifts in Mutation Profiles between Primary and Synchronous Lymph Node Metastases (mLN) in Triple Negative Breast Cancer

Weiqiang Zhao, Kara Patterson, Susan Long, Kevin Y Zhao, Nehad Mohamed, Joshua Coleman, Yan Tang, Bhuvaneswari Ramaswamy, Daniel Jones. The Ohio State University Wexner Medical Center, Columbus, OH; The Ohio State University James Cancer Center, Columbus, OH.

Background: Triple negative breast cancer (TNBC) has been subclassified into multiple distinct immunophenotypic subtypes with variable clinical features. For example, in our previous study, TNBC with overexpression of CD24 in tumor cells and CD10 in tumor stromal cells was associated with both nodal and remote metastases . Prior studies have also shown that TNBC breast biopsies and metastases are molecularly heterogonous (Eur J Hum Genet. 2010,18:560). Given that mLNs are a target for adjuvant therapy, we sought to assess the stability of the mutation profile in primary and metastatic tumors from the same patients.

Design: We studied paired breast primaries and synchronous mLN from 17 TNBC patients (pts, median ages: 51.5 years old). DNA from the paired samples was tested with a clinically-validated next generation sequencing (NGS) assay with 5% sensitivity for missense mutations, assessing mutations in 50 relevant target genes. BRAF V600E mutation was confirmed by Sanger sequencing.

Results: Among the 34 samples from 17 pts, 39 non-synonymous mutations were identified (2.3/pt), including 30 that were present at both sites (concordant). Mutations were seen in TP53 (22/39, 56.4%), BRAF V600E (10%), PIK3CA (10%), MET (8%), APC and KDR in 2 each, and ATM, FGFR3, JAK3 and KIT in one case each. In 6 cases (35.3%), a total of 9 mutations were present in the breast biopsy but absent in mLN. These absent mutations include BRAF (V600E, 4), TP53 (4), PIK3CA (1) and APC (1). The discordant TP53 mutants were p.V274_C275del (2), p.R273H (2), p.E339* (1) and p.H179Q (1). Sanger sequencing of the breast samples in BRAF-mutated cases showed that V600E levels were high in 2 cases and low-level in 2. Discordant mutation status was unrelated to CD10 or CD24 expression but was associated with cases with higher mutation burden (2.83±0.55 versus 1.81±0.77, $p<0.001$).

Conclusions: We noted a 35% incidence of discordant mutation profiles between breast and mLN sites in TNBC that preferentially affected cases with higher mutation burden. TP53 and BRAF V600E mutations were commonly absent in the metastasis, which could potentially affect the clinical management of these pts. Further work is needed to understand whether clonal heterogeneity or adverse selection might be underlying this phenomenon but multisite sequencing approaches may be warranted.

Pediatric Pathology

1830 Collagen XVIII and Procollagen-lysine, 2 oxoglutarate 5-dioxygenase 2 (PLOD2) Expression in Human Pediatric and Mouse Rhabdomyosarcomas: Exploring Potential Biomarkers of Therapeutic Relevance

Jesse Bond, Sakir H Gultekin, Christopher Hartley, Teagan Settelmeyer, Charles Keller, Atiya Mansoor. Oregon Health and Sciences University, Portland, OR; Children's Cancer Therapy Development Institute, Fort Collin's, CO; Medical College of Wisconsin, Milwaukee, WI.

Background: Collagen XVIII (COL18A1) and Procollagen-lysine, 2 oxoglutarate 5-dioxygenase 2 (PLOD2) are recently described proteins associated with increased metastatic and local spread in carcinomas. Our aim is to study expression of COL18A1 and PLOD2 in pediatric rhabdomyosarcomas and mouse model rhabdomyosarcomas which are potential therapeutic targets.

Design: A tissue microarray (TMA) of 74 tumors was constructed with 4 human and 70 murine sarcomas. Human tumors included 4 pediatric rhabdomyosarcomas, including: 3 alveolar and 1 embryonal subtype. The TMA was stained with COL18A1 and PLOD2 immunohistochemistry yielding viable lesion for 47 COL18A1 and 48 PLOD2 cases. The TMA sarcomas are listed in table 1. The lesional cells were scored for intensity of staining (weak, moderate, strong) and percent of positive lesional cells (1-10; 11-50; 51-80; 81-100). In 30 cases, more than one section of viable tumor was available for scoring therefore averages of intensity and total percent were calculated. Any averaging less than 1 (mild) for intensity were scored as no staining.

Sarcoma Subtype	COL18A1 (47)	PLOD2 (48)
Alveolar Rhabdomyosarcoma	16	16
Embryonal Rhabdomyosarcoma	9	9
Pleomorphic Rhabdomyosarcoma	3	7
Mixed Alveolar/Embryonal Rhabdomyosarcoma	1	1
Undifferentiate Sarcomas NOS (plomorphic, spindle, epitheliod)	18	15

Results: 42 of 47 (89.4%) of the sarcomas stained positive for COL18A1, 26(55%) of which had a staining intensity of moderate or greater. The sarcomas that lacked COL18A1 expression were undifferentiated sarcomas NOS (4) and pleomorphic rhabdomyosarcoma NOS (1). 45 of 48 (93.8%) sarcomas expressed PLOD2, 27 (56%) of which had at least moderate staining intensity. The sarcomas that lacked PLOD2 expression were undifferentiated sarcomas NOS (2) and pleomorphic rhabdomyosarcoma NOS (1).

Conclusions: All human and mouse alveolar and embryonal rhabdomyosarcomas expressed significantly increased amounts of PLOD2 and COL18A1 relative to normal background tissue. While this pilot study analyzed only a small cohort of human tumors, it raises the possibility of eligibility for therapies targeting post-translational modifications of collagen, and suggests further human sarcoma subtypes to study for these markers.

1831 Will the Quest for a Novel Positive Marker for a Diagnosis of Hirschsprung Disease on Formalin Fixed Rectal Mucosal Biopsies End with a Glucose Transporter? A Detailed Dual IHC Panel Study of GLUT1 and Calretinin

Maria F Bukelo, Usha Kini, Suravi Mohanty, Kanishka Das. St. John's Medical College and Hospital, Bangalore, Karnataka, India.

Background: Hirschsprung disease (HD) is characterised by the aganglionosis of the rectum and its diagnosis is challenging due to the lack of a specific positive marker on formalin fixed paraffin embedded sections (FFPES) of rectal mucosa. Neither is AChE histochemistry (gold standard for HD diagnosis) suitable for FFPES nor is calretinin IHC, as it is a negative marker. Hence this study, to search for a novel positive IHC marker on mucosal FFPES for a definitive diagnosis of HD.

Design: This cross sectional study was conducted on 20 full thickness FFPES of colon and 20 rectal mucosal biopsies; in 2 phases, each over a period of 6 months. In the first phase, 20 full thickness FFPES from resected ganglionic and aganglionic segments of HD were stained with H&E and GLUT1 (SPM498, Biocare) antibody and compared with the neuronal panel of Calretinin, Synaptophysin, CD56, NF, GFAP, S100 and PGP9.5. These were independently reported by 3 pathologist. The findings obtained were extrapolated to the second phase of the study for ratification, where subsequent 20 consecutive rectal mucosal biopsies, stained with H&E; GLUT1 and calretinin were studied (blind to the final diagnosis) and compared with the corresponding AChE stained sections.

Results: Phase 1: GLUT1 stained the perineurium (PN) of serosal nerves in all segments and the PN of both submucosal and myenteric plexus nerves in aganglionic segments but was absent/minimal in the PN of ganglionic/normal colonic segments; ganglion cells were negative. Phase 2: Of the 20 rectal mucosal biopsies (9 HD and 10 Non-HD cases; 1 case inadequate after FFP embedding) studied, all 9 HD cases were diagnostic on GLUT1 staining which showed strong PN staining of small and large fibres in the submucosa. On the other hand, of the 10 Non-HD cases, 2 cases yielded a false positive diagnosis of HD by showing a strong PN staining of small nerve fibres in the submuscosa. Thus, while the NPV of an independent GLUT1 IHC marker for HD was 100%, its PPV was only 80%. However, when the GLUT1 sections were read with calretinin, a correct diagnosis was obtained in 100% cases as ratified by the AChE staining.

Conclusions: The positive ring-like perineural staining of GLUT1 and negative staining of Calretinin are diagnostic of HD on FFPE rectal mucosal biopsies. A dual panel of GLUT1 and Calretinin IHC stains on FFPES could be as accurate as the gold standard AChE staining on frozen sections for the diagnosis of HD.

1832 A Strategy for Helicobacter Immunohistochemistry Utilization in the Pediatric Setting: Details from a Morphologic and Cost: Benefit Analysis

Miriam Conces, Christina A Arnold, Michael Arnold. Nationwide Children's Hospital, Columbus, OH; The Ohio State University Wexner Medical Center, Columbus, OH.

Background: Dedicated cost-benefit analysis of universal *Helicobacter* immunohistochemical (IHC) staining in pediatric gastric biopsies has not been performed. As such, we undertook a morphologic study of pediatric *Helicobacter* cases with the intent to provide useful guidelines in the pediatric setting.

Design: All *Helicobacter* positive gastric biopsies were retrospectively collected from our primary and referral care center over twelve months (63 cases) and 122 *Helicobacter* negative gastric controls were randomly selected from the same time period. All cases were reviewed and scored according to the Sydney System for the severity of acute and chronic inflammation, as well as the location of inflammation and presence of lymphoid follicles.

Results: Within the reviewed 12 month period 1,979 total pediatric gastric biopsies were identified, including 63 *Helicobacter* positive cases (3.2%). We reviewed 185 biopsies (63 *Helicobacter* positive, 122 *Helicobacter* negative controls) and the corresponding *Helicobacter* IHC, which was performed in all cases. *Helicobacter* infection was significantly associated with lymphoid follicles (cases=42.9% vs. controls=4.1%, $p<0.0001$), active inflammation (cases=84.1% vs. controls=8.2%, $p<0.0001$), moderate or severe chronic inflammation in the oxyntic mucosa(cases=47.6% vs. controls=2.5%, $p<0.0001$) and any chronic inflammation in the antrum except inflammation that was both mild and superficial (cases=95.2% vs. controls=21.3%, $p<0.0001$). At least one of these inflammatory patterns was seen in all *Helicobacter* positive biopsies, compared with 34 of 122 control biopsies (100% vs. 27.9%, $p<0.0001$). Chronic active gastritis was present in 53 *Helicobacter* positive biopsies and 9 control biopsies (84.1% vs. 7.4%, $p<0.0001$).

Conclusions: We recommend performing *Helicobacter* IHC on pediatric gastric biopsies where organisms are not identifiable on H&E sections with any of the following inflammatory patterns: 1) lymphoid follicles, 2) any active inflammation, 3) moderate or severe chronic inflammation within the oxyntic mucosa, or 4) any chronic inflammation in the antrum except mild superficial inflammation. This approach can sensitively identify pediatric patients with *Helicobacter* gastritis while limiting IHC staining to approximately 30% of all gastric biopsies. In comparison with universal *Helicobacter* IHC, this approach would reduce patient charges at our institution by approximately $280,000 per year.

1833 TdT-Positive Cells in Inflamed Pediatric Kidney: A Potential Diagnostic Pitfall

Jennifer Dunlap, Xavier Stacey, Sarah Click, Michael J Cascio, Megan Troxell. OHSU, Portland, OR.

Background: We encountered a patient with infantile nephrotic syndrome associated with a dense mononuclear infiltrate and prominent extramedullary hematopoiesis (EMH). Immunohistochemical analysis revealed numerous Terminal deoxynucleotidyl

Transferase (TdT) positive cells which raised concern for lymphoblastic lymphoma. EMH has been reported in the setting of dysplastic pediatric kidneys; however, to our knowledge, TdT expression has not been studied.
Design: Pathology records were searched for pediatric nephrectomy or autopsy kidneys with inflammation (age 0-21). Slides were reviewed, with attention to EMH. The study group included 39 nephrectomy blocks from 36 patients, and 4 kidney blocks from 4 infant autopsies. Sections were stained for TdT by immunohistochemistry. TdT+ nuclei were quantitated (average of 3 maximal high power fields (hpf)). Dual immunostains for TdT/CD79a, TdT/CD3, and TdT/CD43 were performed in 6 cases with abundant TdT positivity.
Results: TdT+ nuclei were present in 42 of 43 inflamed pediatric kidney blocks. TdT counts ranged from 1 to >200/hpf (mean 44.4). The presence and number of TdT+ nuclei showed a strong association with younger patient age, as did the presence of EMH (Table 1).

Age (years)	N	Average TdT+nuclei/hpf (range	EMH
0-2	23	77.5 (4- >200)	12/23 (52%)
2-10	13	4.7 (1-15)	0/13
10-21	7	9.1 (0-30)	0/7

In patients <2 years old, the presence of EMH did not correlate with TdT count (p=0.108). Kidneys with abundant TdT were heavily inflamed, but dense inflammation did not imply high TdT counts. Dual immunostaining demonstrated that a small subset of TdT+ cells showed co-expression with CD43 and CD79a. Collections of TdT+ cells did not localize in T-cell rich zones, and TdT+ cells were not seen in B-cell follicles or germinal centers.
Conclusions: We show that TdT+ cells are frequently part of the inflammatory milieu in pediatric kidneys, and may be abundant, especially in infants. Focal EMH was seen in half of the inflamed infant kidneys in our series but did not correlate with TdT expression. Most TdT+ cells in kidney showed a null-lineage specific phenotype, with a subset of cells showing expression of CD79a or CD43, suggesting precursor B-cell phenotype in some, as previously reported in pediatric tonsil and lymph node. These findings highlight a potential diagnostic pitfall; while TdT is a robust marker of lymphoblastic lymphoma, caution is needed in small biopsies of infant kidney, as TdT+ cells may be part of the inflammatory milieu.

1834 Juvenile Laryngeal Papillomatosis: Relation between p16 and p63 Expression, Human Papilloma Virus Infection and Clinical Evolution

Louise Galmiche, Sebastien Pierrot, Helene Pere, Vincent Couloigner, Cecile Badoual. Necker Hospital, Paris, France; Georges Pompidou European Hospital, Paris, France.
Background: Juvenile laryngeal papillomatosis (JLP) are benign lesions due to Human Papilloma Virus (HPV) infection, especially low risk HPV. JLP evolution remains unpredictable, varying from spontaneous remission to obstructive life threatening tumor. No data allow predicting the clinical outcome of this condition. We aimed to determine prognostic value of HPV status, immunostaining of P16 and P63 status compared with histological examination.
Design: We performed histological examination, p16 and p63 immunostaining and low risk (LRHPV) and high risk (HRHPV) HPV chromogenic *in situ* hybridization (CISH) in 29 JLP patients (53 biopsies).
Results: Patients were 1 to 21 years old (mean = 7). No or mild dysplasia was observed in 23 patients at diagnosis, and one had severe dysplasia. Twelve patients recurred, 7 having low dysplasia. Only 2 patients had increased degree of dysplasia with recurrences and 3 a decreased one, the 7 other had no modification of dysplasia grade. The 7 multifocal JLP recurred. Over the 17 basal p63 staining, 16 had no or mild dysplasia. However no difference in p63 staining was noted between recurring and non recurring patients. The CISH was negative for 12 of these 17 low grade dysplasia patients. The CISH showed 18 LRHPV and one HRHPV CISH for which P16 staining was positive (high risk dysplasia). No p16 staining was present in other JLP without HPV or with LRHPV.
Conclusions: No or mild dysplasia and LRHPV are usually seen in JLP. Degree of dysplasia seems stable over recurrences. HRHPV is extremely rare and associated to severe dysplasia. The level of p63 expression in the mucosa seems linked to the degree of dysplasia. However p63 status cannot predict recurrences.

1835 Placental Pathology in Small-for-Gestational Age Placentas from Pregnancies with Type 1 Pregestational Diabetes

Mai He, Phinnara Has, Suzanne DeLaMonte, Roman S Starikov. Women Infants Hospital of Rhode Island/Alpert Medical School of Brown University, Providence, RI; Women Infants Hospital of Rhode Island, Providence, RI; Rhode Island Hospital / Alpert Medical School of Brown University, Providence, RI; Phoenix Perinatal Associates, Phonnix, AZ.
Background: Diabetes Mellitus (DM) is one of the most common medical complications of pregnancy. Adverse perinatal outcome associated with pregestational DM include macrosomia and large placentas. While many previous diabetic pregnancy studies focused on the "large" aspects of the adverse outcome, in non-diabetic pregnancies the small-for-gestational (SGA) placentas exhibit increased rates of adverse perinatal outcomes. Current study investigated the clinicopathological correlation in SGA placentas from pregnancies complicated with type 1 DM (T1DM).
Design: In this retrospective cohort study, we identified the subject population using registration statistics for the (state) Diabetes in Pregnancy Program (2003 to 2011). SGA is defined as < 10th percentile while appropriate-for-gestational age (AGA) as 10-90th percentile. Categorical variables were compared by Chi-square[1] or Fisher's exact test[2], and continuous variables were compared using t-test[3]. P<0.05 was considered statistically significant.
Results: 117 placentas from women with T1DM were identified, including 22 (18.9%) SGA and 63 (53.8%) AGA placentas. The placental weight and neonatal weight were significantly lower in the SGA group (P<0.0001) while the fetal-to-placental (f/p) weight ratio higher (P=0.03). The GA at delivery was significantly lower with SGA placentas (P=0.02). 12 (54.6%) SGA placentas were associated with f/p ratio > 90%tile, suggestive of exhausted placental functional reserve. There were more IUGR associated with SGA placentas (P=0.04). Histologically, there was more thrombosis of fetal vessels in the SGA placentas (P=0.004), suggestive of higher prevalence of fetal thrombotic vasculopathy. The SGA group had the only stillbirth case although statistical significance not reached (1/22 vs 0/63, P=0.26).
Conclusions: SGA placentas are associated with significantly increased rates of IUGR, more f/p ratio > 90th percentile and thrombosis of fetal blood vessels in placenta. The adverse outcome can include stillbirth. Further research is needed to elucidate mechanisms and consequences of SGA placenta and fetal circulation in T1DM. Closer attention should be given to gravida with T1DM and smaller placenta.

1836 Frequent HRAS Mutations in Ectomesenchymoma (ECM): Overlapping Genetic Abnormalities with Embryonal Rhabdomyosarcoma (ERMS)

Shih-Chiang Huang, Rita Alaggio, Yun-Shao Sung, Narasimhan P Agaram, Cristina Antonescu. Memorial Sloan Kettering Cancer Center, New York, NY; Chang Gung Memorial Hospital, Taoyuan, Taiwan; Padova University Hospital, Padova, Italy.
Background: ECM is an exceedingly rare pediatric sarcoma exhibiting a predilection for infants and young children. Microscopically the tumors harbour a biphasic phenotype composed of rhabdomyosarcoma (RMS) and a ganglioneuroma component. Although ECM is considered a neuroectodermal neoplasm with rhabdomyoblastic elements and classified under malignant nerve sheath tumors in the latest WHO, it remains unclear if its biology and clinical behaviour are closer to ERMS or malignant peripheral nerve sheath tumors (MPNST).
Design: In this study we sought to investigate the genetic abnormalities of ECM and subjected 2 index cases to RNA sequencing. FusionSeq and Mutation detection algorithms for novel fusion gene discovery and oncogenic driver mutations, respectively, were applied. No fusion candidates were identified; but a recurrent pattern of mutations was noted which was then screened in 5 additional ECM cases. A control group of ERMS matched for age was tested for the same abnormalities. As the majority of MPNST show loss of H3K27me3 expression by IHC, we also assessed this marker in the ECM cohort.
Results: All 7 ECM patients were male, with a mean age at diagnosis of 7.5 months (range 0.6-17 mo). All except one occurred in the pelvis/paratesticular region; one case arose in the hand. All cases showed a RMS component (positive for desmin, myogenin), which ranged from typical embryonal, spindle cell and occasionally undifferentiated/round cell phenotype. The neuroectodermal elements (positive for S100, synaptophysin) were represented by scattered ganglion cells or areas of ganglioneuroma. Recurrent *HRAS* and *PTPRD* mutations were identified in both index cases, with one case also harbouring *FBXW7* mutations. By Sanger sequencing, 6/7 (86%) cases had *HRAS* mutations (4, p.G13R; 2, p.Q61L) and 2 cases had *PTPRD* mutations. No additional cases showed *FBXW7* mutations. No *EED/SUZ12* mutations, typically seen in MPNST, were detected by RNAseq and H3K27me3 expression was retained. In the control ERMS group, 5/9 (56%) showed *RAS* mutations, equally distributed among *HRAS*, *NRAS* and *KRAS* hot spots. The available clinical data in 4 ECM patients showed long term uneventful survival (3-16 years) s/p RMS chemotherapy protocol.
Conclusions: ECM shares frequent *RAS* mutations with ERMS of young age and retains H3K27me3 expression, suggesting a closer genetic link to RMS rather than MPNST. The good response to RMS chemotherapy and long survival corroborates this notion.

1837 Prenatal Jarcho-Levin Syndrome

Ana Larque, Mar Bennasar, Paola Castillo, Alfons Nadal. Hospital Clinic, Barcelona, Spain; Barcelona Center for Maternal-Fetal Medicine and Neonatology, Hospital Clínic, Barcelona, Spain.
Background: Jarcho-Levin syndrome is an eponym that has been used to describe a variety of clinical phenotypes consisting of short-trunk dwarfism associated with rib and vertebral anomalies. In this study, we show the longest prenatal series with Jarcho-Levin syndrome.
Design: We retrospectively reviewed our institution's 2002-2014 prenatal autopsy and respective medical records for fetus with a Jarcho-Levin syndrome. Fetus history, autopsy and radiographic findings were recorded.
Results: Ten fetal autopsies were identified. The fetuses were 7(70%) males and 3(30%) females with a median weeks' gestation of 21 (range, 14-25). Two cases were not identified in the ultrasound antenatal diagnosis. Eight were spondylocostal dysostosis and 2 cases presented some bilateral and symmetrical fusion of the ribs at the costo-vertebral junction resulting in small thoracic volume and limited chest expansion that could correspond to a spondylothoracic dysplasia. Common autopsy findings include short necks, failure of formation and segmentation of vetebral bodies, and rib anomalies. Two cases presented a single umbilical artery. Seven cases were associated with congenital defects of which the most prevalent was renal anomalies.
Conclusions: Advancements in prenatal medicine allow early diagnosis to provide appropriate genetic counseling. More studies are necessary to try to classify Jarcho-Levin syndrome at this early age.

Table 1. Clinical findings

Patient number	Gestational age	Sex	Subtype	Neural tube defects	Associated anomalies
1	21	M	SCD		Renal anomalies
2	23	F	SCD		Single umbilical artery
3	21	F		Myelocele with lumbar-sacral rachischisis, Arnold-Chiari malformations	
4	25	M	SCD		
5	14	M	SCD		
6	21	M	SCD	Spina bifida occulta	Esophageal atresia with distal tracheoesophageal fistula, Renal fusion
7	22	M	STD*		
8	21	F	STD*	Spina bifida occulta	
9	21	M	SCD		Single umbilical artery, Renal fusion
10	19	M	SCD		Hypoplasia of the sacrum and lumbar vertebrae, Anal displacement, Renal fusion

SCD, spondylocostal dysostosis; STD, spondylothoracic displasia.
* Clinical and radiographic findings compatible with STD

1838 Absence of Distinct Immunohistochemical Distribution of Annexin A5, C3b, C4d and IgG in Placentas from Patients with Antiphospholipid Antibodies Compared to Preeclampsia and SLE

Cathleen Matrai, Jacob H Rand, Rebecca Baergen. NYPH-Weill Cornell, NYC, NY.

Background: In pregnancy, the presence of preeclampsia (PE), systemic lupus erythematosus (SLE), and/or antiphospholipid antibodies (aPLA) is characterized by poor obstetric outcomes, with potential adverse effects for both the mother and fetus. While the histopathologic changes observed in these entities have been well established, the pathogenic mediators associated with tissue injury are poorly understood. The goal of this study was to investigate immunohistochemical (IHC) staining patterns in placentas of patients with PE, SLE, and aPLA using a panel of complement activation products and inflammatory biomarkers.

Design: 40 placentas were evaluated, including 10 patients with a history of preeclampsia, 10 with SLE, and 10 with documented aPLA. 10 disease-free controls were selected based on an unremarkable clinical history and the absence of pathologic findings in the placenta. Multiple gestation pregnancies were excluded. Slides were reviewed and histology confirmed. Each case was evaluated with a panel of IHC markers including C3b, C4d, Annexin A5 (A5), and IgG. Staining was graded on intensity (0, 1+, 2+, 3+) and distribution (absent, patchy, diffuse).

Results: C4d staining showed a distinct difference between disease groups and controls. 6/10 PE patients showed at least weak, focal staining for C4d, with 1 case showing near diffuse staining. 4/10 SLE patients showed at least weak, focal staining for C4d, with 1 case being strongly positive. 2/10 aPLA cases showed at least focal staining. All controls were negative. A5 staining showed intrinsic variability in all disease groups, while 10/10 controls showed diffuse, strong staining (2+ or 3+). C3b staining was variable within all groups but showed stronger staining in a larger number of cases in disease groups than controls. IgG staining did not show any significant difference among groups.

Group (n=10)	**A5 (loss)**	**C3b (2-3+)**	**C4d (positive)**	**IgG (positive)**
PE	5/10	9/10	6/10	9/10
SLE	6/10	9/10	4/10	10/10
aPLA	2/10	8/10	2/10	10/10
Controls	0/10	5/10	0/10	10/10

Conclusions: Previously, aPLA-associated pregnancy complications have been thought to be a consequence of a unique aPLA-mediated pathogenic mechanism. However, the similarity of the IHC findings in aPLA placentas to those from SLE and PE patients - i.e. increased complement deposition and decreased A5 staining - suggests that aPLA-associated pregnancy complications may reflect a more general autoimmune mechanism, such as localized deposition of immune complexes.

1839 SOX10 Distinguishes Pilocytic and Pilomyxoid Astrocytomas from Ependymomas but Shows No Differences in Expression Level in Ependymomas from Infant Versus Older Children or between Molecular Subgroups

Abby M Richmond, Andrew M Donson, Nicholas K Foreman, Bette K Kleinschmidt-DeMasters. University of Colorado, Aurora, CO; Children's Hospital Colorado, Aurora, CO.

Background: SOX10, a developmentally-regulated transcription factor with Olig 2 interaction, is important in non- neoplastic oligodendroglial development; mRNA transcripts and protein expression are, however, identified in a wider variety of central nervous system glial neoplasms than oligodendrogliomas. We previously showed by Affymetrix and Western blot analyses that high levels of SOX10 mRNA and protein exist in pilocytic astrocytomas (PA), but not ependymomas (EPN). We now extended these studies to investigate subsets of these two tumors known to affect infants: pilomyxoid astrocytomas (PMAs) and ependymomas <age 1 (iEPN), all EPN group A. We hypothesized that SOX10 transcripts might be lower in these generally more-aggressive tumors that affect infants.

Design: Ten PMAs and 6 iEPN were compared with 21 PAs and 52 EPNs, groups A & B, supratentorial and myxopapillary in children >age 1.

Results: iEPNs and all EPNs in older children showed very low SOX10 expression levels, on average 7.1-fold below normal control tissues. EPN groups showed no significance in SOX10 expression between iEPN and EPN. PAs/PMAs had 24.1 /29.4-fold higher transcript levels, respectively, than normal tissues.

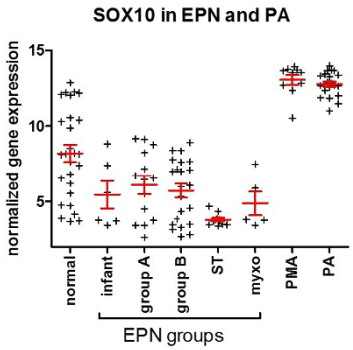

Recognizing the diagnostic potential this offered for distinguishing PA/PMA from EPN in clinical practice, we then applied SOX10 immunohistochemistry to PMAs, PAs, iEPNs, and EPNs from various anatomical sites, including adults to broaden the application. All PA/PMAs but none of 34 iEPNs/anaplastic supratentorial/spinal cord/posterior fossa/myxopapillary/subependymomas showed diffuse nuclear IHC+.

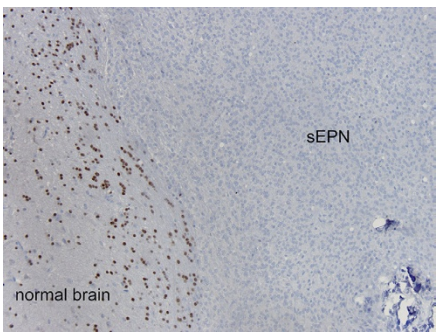

Conclusions: Nuclear SOX10 IHC+ has significant diagnostic utility in distinguishing between PA and PMA from EPN, but does not differentiate infantile subtypes from similar tumors in older children.

1840 BRAF Reactivity and BRAF Mutations in Pediatric Langerhans Cell Histiocytosis

Essia Saiji, Christelle Cerato Biderbost, Margaret Berczy, Anne-Laure Rougemont. Geneva University Hospitals, Geneva, Switzerland.

Background: Langerhans cell histiocytosis (LCH) has a wide age range distribution, with a peak incidence in children aged 1-3 years old. Mutations in the *BRAF* gene have been described in LCH with an overall frequency of 48.5%, lending support to a neoplastic origin. *BRAF* activating mutations induce in mutated cells senescence pathways; in particular intense expression of the cell-cycle gatekeeper $p16^{INK4a}$ has been shown in this setting. We assessed the expression of BRAF and senescence markers in a series of pediatric LCH, and compared the BRAF immunohistochemistry (IHC) results with Next Generation Sequencing (NGS) findings.

Design: Twelve LCH cases from patients aged 2 to 17 years old (median 59 months) were sub-cutaneous in 4 patients, and located in bone in 8 patients. For IHC, we used the BRAF (V600E, Spring), $p16^{INK4a}$ (ref. 805–4713, Ventana), and $p21^{CIP1/WAF1}$ (SX118, DAKO) antibodies. Staining intensity was evaluated semi-quantitatively, and the percentage of positive LCH cells was determined. NGS was performed on DNA extracted from paraffin blocks using the Ion AmpliSeq™ Cancer Hotspot Panel v2 (Thermo Fisher), covering approximately 2,800 COSMIC mutations from 50 oncogenes and tumor suppressor genes. Variant analysis was performed using the "Gensearch NGS" software (Phenosystems). Tumor content varied from 30% to 90%. TaqMan assay was performed in one tumor where DNA amount was not sufficient for NGS Analysis.

Results: Intense BRAF reactivity (2+ or 3+, in 80% to 100% tumor cells) was seen in 4 tumors, 3 of which occurring in bone. In all 4 tumors, NGS confirmed the presence of a *BRAF* V600E mutation, in a proportion of the tumor cells ranging from 15% to 70%. A further tumor showing no BRAF reactivity displayed a V600D *BRAF* mutation. Senescence associated proteins p16 and p21 showed reactivity in all tumors. Intense 3+ p16 nuclear reactivity was seen in 60% to 100% of the LCH cells, whereas p21 nuclear reactivity was of variable intensity (1+ to 3+), staining only a minority of the LCH cells (from 1% to 30%).

Conclusions: In all 12 tumors correlation was observed between BRAF IHC findings and *BRAF* mutation status. Interestingly, the only patient displaying no BRAF IHC reactivity despite *BRAF* mutation showed a V600D mutation, in keeping with antibody

specificity for V600E. Senescence associated protein (p16 and p21) reactivity was observed in all tumors, independent of the *BRAF* mutational status. Therefore, mechanisms other than oncogene-induced senescence are likely to be involved.

1841 Botryoid Wilms Tumor: A Non-Existent "Entity" Causing Diagnostic and Staging Difficulties

Marco Schiavo Lena, Gordan Vujanic. San Raffaele Scientific Institute, Milano, Italy; University Hospital of Wales, Cardiff, United Kingdom.

Background: Wilms tumors (WTs) growing in a botryoid fashion into the renal pelvis have been reported since the late 1960s as a rare tumor type associated with stromal histology (so-called *Fetal Rhabdomyomatous Nephroblastoma, FRN*) and a good prognosis. However, its true frequency, association with WT subtypes and stage have never been comprehensively studied.

Design: All renal tumors enrolled into the SIOP UK 2001 Trial (2001 – 2011) were retrieved. Gross and microscopic findings (botryoid growth) were evaluated in all cases and correlated with histology and stage

Results: Out of 847 pediatric patients with renal tumors, there were 739 WTs, and 77 (10.7%) of them showed a botryoid pattern. There were 41 males and 36 females. The mean age was 39 months (from 4 to 172) versus 44 months of the whole WT group. One patient had Denys-Drash syndrome. In 43 patients tumor was in the left, in 35 in the right and one in a horseshoe kidney. WTs were sub-classified according to the SIOP criteria as follows: 29 tumors were stromal type (FRN in 17 cases), mixed type in 22, regressive in 7, completely necrotic in 3, blastemal in 4, epithelial in 2, diffuse anaplasia in 2 and non-anaplastic type (surgery first) in 10. Stage was as follow: stage I 26 cases, stage II in 24, stage III in 12, stage IV in 9 and stage V (bilateral) in 6, 2 of which displayed botryoid growth in both kidney. In 6 cases the local pathologist upstaged wrongly the tumor from stage I to stage II because of the botryoid growth itself. ILNRs were found in 22 cases, PLNRs in 12, 4 patients had both ILNRs and PLNRs.

Conclusions: Botryoid growth pattern is a relatively common finding in WT (about 10% in our large series). All histological types of WT can share this feature, and it appears in all stages. In the SIOP and COG staging criteria, the botryoid growth itself is not a criterion for stage II. The botryoid WT is not an entity but a pattern of tumor growth and these tumors should be sub-classified according to their overall histological features, which will determine treatment and prognosis.

1842 High Level Expression of Divergent Endodermal Lineage Markers in Gonadal and Extragonadal Yolk Sac Tumors

Hadi Shojaei, Hong Hong, Raymond W Redline. University Hospitals Case Medical Center, Cleveland, OH.

Background: Yolk sac tumors (YST), either pure or mixed with other elements, can occur in both gonadal and extragonadal (EG) sites. Divergent expression of endodermal lineage markers (ELM) may lead to delayed diagnosis as exemplified by a recent case of ovarian endometrioid-pattern YST with strong diffuse expression of TTF-1. The aim of this study was to assess the frequency, extent, and pattern of expression of three divergent ELM, TTF-1, CDX-2, and Hep-PAR1, in ovarian (OV), testicular (T), and EG YST before and after puberty.

Design: All gonadal and EG YST from 1999-2013 were retrieved (N=26). Cases were separated by site (OV=5, T=15, EG=6) and age (prepubertal: EG=5, T=1, postpubertal: T=14, OV=5, EG=1). YST areas were defined as SALL-4+/Oct-4-. Relative proportion of 4 histologic patterns: microcystic, papillary, solid/myxoid, and glandular (enteric or endometrioid) was estimated. No polyvesicular vitelline or hepatoid foci were seen. Percent positivity for AFP, GLYP-3, TTF-1, CDX-2, and Hep-PAR1, was compared within YST areas according to site, age group, and histologic pattern.

Results: The majority of YST (16/26) showed a predominance of the microcystic pattern. Most of the remaining YST had no predominant pattern. Testicular YST were all mixed type while 8/11 tumors from other sites were pure YST. All YST expressed AFP and GLYP-3. Mean percent positivity of AFP was highest in prepubertal YST (43% vs 18%) while mean percent positivity for GLYP-3 was uniform in all groups (~33%). High level (>25%) positive staining (HL+) for one or more divergent ELM was seen in 16/26 YST. HL+ TTF-1 was only seen in EG and OV YST (2/5 each), while HL+ Hep-PAR 1 staining was restricted to postpubertal tumors (8/20). HL+ CDX-2 staining (n=3) showed no age or site predilection. No case was HL+ for all 3 divergent ELM. Two cases were HL+ for TTF-1 and Hep-PAR 1 (both OV). One case was HL+ for TTF-1 and CDX-2 (EG) and one HL+ for CDX-2 and Hep-PAR 1 (T). No consistent pattern of divergent ELM expression by histologic pattern was observed. However, HL+ TTF-1 or CDX-2 expression was never seen in myxoid/solid areas and HL+ HepPAR-1 was predominantly observed in myxoid/solid and glandular areas.

Conclusions: High level expression of one or more divergent ELM is seen in a majority of YST. Hep-PAR 1 positivity is less commonly used to interrogate tumors of unclear origin, but expression of TTF-1 and CDX-2 may create diagnostic confusion when not combined with other YST markers, particularly SALL-4.

1843 Targeted Sequencing Analysis of Aggressive Pediatric Rhabdomyosarcomas

Olivia L Snir, Farzana D Pashankar, Zenta Walther, Karin E Finberg, Jeffrey L Sklar, Raffaella Morotti. Yale University School of Medicine, New Haven, CT.

Background: Even with current therapy, metastatic rhabdomyosarcoma (RMS) shows a poor 5-year survival of only 30%. To search for potentially actionable mutations in FFPE tumor specimens, we have employed a targeted next-generation sequencing (NGS) panel.

Design: Six cases of aggressive RMS were selected (ages: 2-20 yrs); 4 were metastatic at presentation and the others developed metastases within two years. Four cases harbored a *PAX3-FOXO1* gene fusion characteristic of alveolar RMS. For each case, tumor and control tissues were analyzed in parallel. Sequencing was performed in a CLIA laboratory, using a panel of 409 cancer-related genes (~98% exon coverage).

Results: Multiple mutations and gene amplifications were identified (Table 1). *MYCN*, *MDM2*, and *CDK4* amplifications were each seen in 50% of our fusion positive cases, and no amplifications were detected in either fusion negative case. Both patients with fusion positive tumors showing high level gene amplifications (ploidy 10) suffered a fulminant course. Mutations in the RTK/RAS/PI3K pathway were identified only in fusion negative cases. A *TP53* mutation was seen in a fusion positive tumor.

Conclusions: In accordance with previous studies, we found that tumors positive for *PAX3* gene fusion showed amplification of cell cycle regulatory genes, whereas fusion negative tumors had mutations in the RAS/PI3K pathway. Remarkably, a potentially actionable alteration was found in every tumor – a high yield relative to reports of NGS in other tumor types. Our study shows that molecular profiling of RMS in a clinical setting is feasible, may yield prognostically useful information, and ultimately can guide treatment of this devastating disease.

Age / Gender	Metastatic at Presentation	Time to Relapse	Outcome (Survival)	PAX3 Gene Fusion	Tumor Tissue Analyzed^	Driver Mutations	Amplifications (ploidy)
15 yo F	Yes	Persistent disease	DOD* (10 mo)	Yes	M	*TP53*	*MYCN*(10)
16 yo M	Yes	16 mo	DOD* (25 mo)	Yes	M	-	*CDK4*(10)
17 yo F	Yes	22 mo	Alive (at 38 mo)	Yes	P	-	*ERBB3*(4), *CDK4*(4), *MDM2*(4), *MYCN*(4)
6 yo M	Yes	No recurrence	Alive (at 11 mo)	No	P	*PIK3CA*	-
20 yo F	No	15 mo	Alive (at 26 mo)	Yes	M	-	*MDM2*(6)
2 yo F	No	19 mo	Alive (at 69 mo)	No	M	*NF1*, *PTPN11*	-

*DOD=Died of Disease
^P=Primary Site, M=Metastasis

1844 Molecular Characterization of Gliomas in Adolescents and Young Adults

Mariona Sunol, Josep Riera Monroig, Carmen de Torres, Iban Aldecoa, Carlota Rovira, Cristina Jou, Eva Rodriguez, Ofelia Cruz, Teresa Ribalta. Hospital Sant Joan de Deu, Barcelona, Spain; Hospital Clinic, Barcelona, Spain.

Background: Pediatric and adult gliomas show substantial differences in clinical behavior and molecular aberrations. However, the molecular definition of gliomas in the transition from pediatrics to adulthood has not been established. The aim of our study was to determine the frequency of molecular alterations in adolescents and young adults to identify a limit age where molecular profile is characteristic of pediatric or adult gliomas.

Design: This cohort included 47 gliomas diagnosed in adolescent and young adult patients aged 12 to 36 years. All glioma subtypes (except ependymoma) and WHO grades were included, being 44.4% high-grade gliomas (HGG). Molecular analysis included Sanger sequencing (*IDH1*^{R132H}, *BRAF*^{V600E}, *H3F3A K27M)*, RT-PCR (*KIAA1549-BRAF)*, immunohistochemistry (P53, IDH1, K27M, EGFR), MSPCR *(MGMT*) and FISH (1p/19q codeletion). Statistical associations between molecular results and histological subtype, WHO grade, patient age and other relevant clinical variables were assessed.

Results: IDH1^{R132H} mutation was found in 22.6% of cases (3 low-grade and 4 HGG). IDH1 correlated with *TP53*mutation (p=0.013) and was associated with worse OS (p=0.045). All patients with IDH1-mutated gliomas were older than 23. *TP53* was present in 29.7% of tumors and was associated with HGG (p=0.044) and worse outcome (p=0.001). Mutation of *TP53* was present in the 4 glioblastomas (GB). *MGMT* was identified in 3/7 HGG. 1p/19q codeletion was found in 1 of the 10 oligodendrogliomas. BRAF^{V600E} was present in 17.2% of tumors. *KIAA1549-BRAF* was identified in 3 out of 7 pilocytic astrocytomas. H3F3A K27M was not found in any of the 8 HGG studied (none in the midline).

Conclusions: The high prevalence of IDH1^{R132H} and TP53 mutations observed in the HGG of this series of adolescent and young adult patients suggest that these tumors are molecularly closer to secondary adult GB. IDH1 was not found in patients before the age of 23. No age threshold could be determined in this series due to heterogeneity of subgroups and limited sample size. A larger cohort of patients covering the ample range of age from adolescent to young adults is required to establish the molecular definition of these tumors.

1845 Clinicopathological Study of Hepatoblastoma with Pulmonary Metastases

Mio Tanaka, Misa Yoshida, Rieko Ijiri, Norihiko Kitagawa, Masato Shinkai, Hiroaki Goto, Yukichi Tanaka. Kanagawa Children's Medical Center, Yokohama, Japan.

Background: For hepatoblastoma (HBL) patients with pulmonary metastasis, good prognosis may be obtained by complete metastasectomy. On the other hand, there are patients with frequently recurring metastases resulting in poor prognosis.

Histopathological study on metastatic lesions of HBL has not been carried out sufficiently so far. We examined the clinicopathological features of primary and metastatic lesions of HBL to clarify the characteristic histology of metastatic lesions with multiple recurrences.
Design: Seventeen HBLs with pulmonary metastasis/metastases were collected from archives of our institute. Histological review of subtype of both primary and metastatic lesions and a retrospective chart review of patients were carried out.
Results: There were 11 boys and 6 girls. Average age at surgery were distributed between 1 year to 13 years. Nine patients were alive without disease, four were under treatment, and four were dead by disease. Histological specimens of the primary lesion after chemotherapy were available in 8 cases; four showed epithelial component only, and the remaining four showed mixed epithelial and mesenchymal components including osteoid formation. Metastasectomy was carried out 62 times in total (1-8 times/patient), and 336 pulmonary metastatic lesions were submitted (1-27 lesions/one operation). Osteoid was found in the metastatic lesions of three patients, and in the other patients, the metastatic lesions were composed of only epithelial component. Most of the epithelial component were embryonal type. In five cases, epithelial component with fetal type was observed in the initial metastasectomy; however, only embryonal type was observed in the specimen of recurrent metastasis. The metastatic lesions with osteoid have not recurred after the initial metastasectomy. Nests or aggregates of small round cells with marked nuclear expression of beta-catenin, low proliferative activity, and few differentiating features toward hepatocyte, were observed in four cases. All patients with metastatic lesions with osteoid formation were alive without disease. Four of five patients with metastatic lesions showing fetal type epithelial component were alive without disease, and one patient was under treatment.
Conclusions: Frequently recurring metastatic lesions were mostly composed of embryonal type epithelial component, and small round cells without overt differentiation toward hepatocyte were observed in some of these lesions. On the other hand, cases with metastatic lesions with osteoid formation or those composed of fetal type epithelial component showed good prognosis.

1846 Reevaluation of Histological Features for Intra/Extra Pulmonary Sequestration

Mio Tanaka, Rieko Ijiri, Kumiko Nozawa, Noriko Aida, Masato Shinkai, Yukichi Tanaka. Kanagawa Children's Medical Center, Yokohama, Japan.
Background: Definition and classification of cystic lung diseases have been problematic with many overlaps in terminology. For intrapulmonary sequestration (IPS), diverse entities have been included because at present, its diagnosis is mostly dependent on the presence of feeding vessels. Additionally, relatively common occurrence of cystic adenomatoid features mimicking congenital pulmonary airway malformation, type 2, in pulmonary sequestration (PS) has led to case reports of "hybrid lesion", further complicating its definition. The aim of this study was to examine detailed histological features of pediatric PS at our institute and to clarify the spectrum of its histological findings.
Design: During the period from 1970 to 2015, 136 pulmonary lesions submitted for pathological diagnosis at our institute were reviewed. Histological criteria for PS included aberrant elastic-type feeding artery, atretic ectopic bronchial tree, and ectopic hilar tissues (cartilage, mixed respiratory glands, lymph nodes). In addition, morphometric analyses of areas with cystic adenomatoid feature were carried out by using digital scanning system. Retrospective chart review of patients with histologically diagnosed PS were carried out.
Results: In 21 of 136 pulmonary lesions, microscopic examination revealed aberrant elastic-type feeding artery and atretic ectopic bronchial tree near the entry of the feeding artery; 13 were intralobar (IPS) and 8 were extralobar lesions (EPS). Cartilage and/or mixed respiratory glands were noted around the elastic artery forming ectopic hilar tissues in 11 of 13 IPS and all 8 EPS. In 3 IPS, lymph nodes were present. Cystic adenomatoid features were observed in 17 of 21 PS cases (81%). Among 13 digitally scanned PS cases, 9 contained cystic adenomatoid features, ranging from 6% to 57% of the total area of PS in maximal cut section. The age of these patients at surgery ranged from 9 days to 14 years, and there were 10 boys and 11 girls. All patients except one girl were preoperatively diagnosed as PS on imaging study by the presence of feeding artery. In one exceptional patient, no feeding artery, but a cord-like substance, was identified on preoperative imaging study and during operation. Preoperative diagnosis for this patient was bronchial atresia.
Conclusions: By thorough histological examination, the diagnosis of PS is possible even if the lesions show extensive inflammatory changes or have no overt feeding artery on imaging study. The present study showed the importance of ectopic atretic bronchial system and ectopic hilar tissues, which may be used to differentiate IPS from etiologically different ones.

1847 Tracheal Fibromas Represent β-Catenin-Mediated Fibroproliferative Disease

Henry Tran, David Parham. Children's Hospital Los Angeles, Los Angeles, CA.
Background: Tracheal fibroma is a benign mesenchymal proliferation often occurring in children following tracheostomy placement. Although common in older literature, tracheal fibroma is rarely mentioned in recent decades, and many cases with a clinical diagnosis commonly show only granulation and reactive fibroblastic tissue. More polypoid and nodular lesions have been thought to represent fibromatosis, benign fibrous histiocytoma, myofibroblastic proliferations, or even low-grade fibrosarcoma. This study attempts to further characterize tracheal fibromas through current morphologic classification and immunohistochemical analysis.
Design: Our institutional records contained 75 cases of tracheal excision specimens diagnosed with terms related to fibroma, fibrosis, or scarring. Cases were reviewed by the authors, and those showing only granulation tissue were excluded. The 51 remaining cases showed a range of fibroproliferative histology. Sixteen representative nodular cases, with cellular fascicular whorls resembling hypertrophic scar, from 15 patients were selected for immunohistochemical analysis with β-catenin, smooth muscle actin (SMA), desmin, and CD34.
Results: Studied cases included 9 boys and 6 girls (mean age 7.9 years, range 1-20 years). Seven patients had congenital disorders of various types. Fifteen of 16 cases (94%) showed nuclear β-catenin positivity in areas corresponding histologically to spindle or stellate shaped cells arranged in poorly circumscribed whorls and short fascicles. This pattern composed the lesional tissue focally or almost entirely. SMA was restricted to areas of β-catenin positivity and stained less diffusely. Desmin was near absent, staining focally only in cases with predominant β-catenin positive areas. CD34 was negative in all β-catenin-positive areas, but highlighted adjacent mesenchyme. All cases were associated with tracheostomy, and 6 cases recurred after initial excision.
Conclusions: The tracheal lesions in this study demonstrated a fibroproliferative appearance indicative of a hypertrophic scar. Nuclear expression of β-catenin places these lesions in the spectrum of known hypertrophic scarring processes related to β-catenin dysregulation. Associated SMA expression is consistent with a wound healing process, whereby fibroblasts assume a myofibroblastic phenotype. The pattern of CD34 confirms previous findings for fibroproliferative lesions related to scarring. Awareness of these features should be considered to avoid misdiagnosis of desmoid tumor or dermatofibrosarcoma protuberans.

1848 Tight Junction Dysregulation Is Involved in the Rotavirus Infection Related Diarrhea

Richard L Wu, Artur Rangel, Monica Garcia, Janet M Poulik. Jackson Memorial Hospital/University of Miami, Miami, FL; Detroit Medical Center/Wayne State University, Detroit, MI.
Background: Rotavirus infection remains the most common cause of hospitalization and mortality in children due to the severe diarrhea and dehydration and causes more than 600,000 children deaths yearly worldwide. Net fluid loss caused by increased transport of sodium and chloride across the apical membrane of the gut lumen is well documented in the animal model of viral enteritis. However, the role of tight junction disruption and paracellular permeation in human rotavirus infection remains poorly understood. In this study, we measured the expression of tight junction associated proteins in vivo from rotavirus infected patients.
Design: Eight patients were identified clinically and specimens were retrieved through copath from a period between 1984 to 2014 in the department of pathology, Wayne state University. Age matched normal colonic and small intestinal specimens were used as controls. Immunohistochemical stains against tight junction associated proteins claudin-8, myosin light chain kinase (MLCK), and phosphorylated light chain (p-MLC) were performed. The non-parametric Mann-Whitney analysis were employed to assess the IHC intensity scoring data.
Results: Claudin-8 expression was significantly decreased in the small intestine of rotavirus infected patients when compared to the normal cohort ($p<0.05$). However, expression in the colon although downregulated was not statistically significant. MLCK and p-MLC expression were increased in the small intestine and colon in patients with rotavirus infection however not clinically significant.

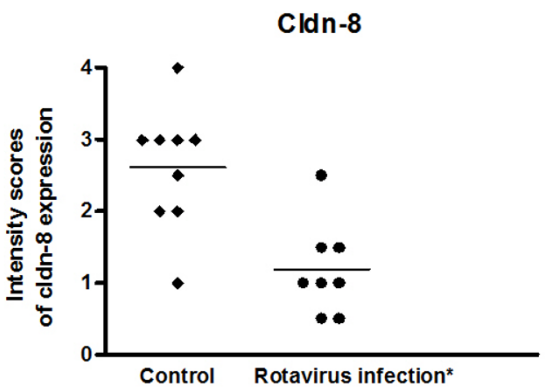

Figure 1: Expression of claudin-8 is significantly decreased in votavirus infected patient *p<0.05

Conclusions: Claudin-8 expression is significantly decreased in the small intestine of patients with rotavirus infection which may indicate that tight junction dysregulation and disruption of paracellular permeation mediates rotavirus related diarrhea.